

NASA Lewis advanced individual pressure vessel (IPV) nickel/hydrogen technology

John J. Smithrick and Doris L. Britton

National Aeronautics and Space Administration, Lewis Research Center, Cleveland, OH 44135 (USA)

Abstract

Individual pressure vessel (IPV) nickel/hydrogen technology was advanced at NASA Lewis and under Lewis contracts. Some of the advancements are as follows: (i) to use 26% KOH electrolyte to improve cycle life and performance; (ii) to modify the state-of-the-art cell design to eliminate identified failure modes and further improve cycle life, and (iii) to develop a lightweight nickel electrode to reduce battery mass, hence reduce launch and/or increase satellite payload. A breakthrough in the Low-Earth-Orbit (LEO) cycle life of individual pressure vessel nickel/hydrogen battery cells was reported. The cycle life of boiler plate cells containing 26% KOH electrolyte was about 40 000 accelerated LEO cycles at 80% depth-of-discharge (DOD) compared with 3500 cycles for cells containing 31% KOH. Results of the boiler plate cell tests have been validated at Naval Weapons Support Center, Crane, IN. Forty-eight Ah flight cells containing 26 and 31% KOH have undergone real time LEO cycle life testing at an 80% DOD, 10 °C. The three cells containing 26% KOH failed on the average at cycle 19 500. The three cells containing 31% KOH failed on the average at cycle 6400. Validation testing of NASA Lewis 125 Ah advanced design IPV nickel/hydrogen flight cells is also being conducted at Naval Weapons Support Center, Crane, IN under a NASA Lewis contract. This consists of characterization, storage, and cycle-life testing. There was no capacity degradation after 52 days of storage with the cells in the discharged state, on open circuit, 0 °C, and a hydrogen pressure of 14.5 psia (1 atm). The catalyzed wall wick cells have been cycled for over 22 694 cycles with no cell failures in the continuing test. All three of the noncatalyzed wall wick cells failed (cycles 9588, 13 900 and 20 575). Cycle-life test results of the Fibrex nickel electrode has demonstrated the feasibility of an improved nickel electrode giving a higher specific energy nickel/hydrogen cell. A nickel/hydrogen boiler plate cell using an 80 mil (2 mm) thick, 90% porous Fibrex nickel electrode has been cycled for 10 000 cycles at 40% DOD.

Introduction

The state of development of individual pressure vessel nickel/hydrogen battery cells is such that they are acceptable for geosynchronous orbit (GEO) applications since not many cycles are required over the life of the battery system (1000 cycles, 10 years). There are 20 communication satellites in GEO using IPV nickel/hydrogen batteries [1]. For the demanding Low-Earth-Orbit (LEO) applications, however, the current cycle life at moderate-to-deep depths-of-discharge (DOD) (40 to 80%) should be improved. Battery cycle life has a major impact on life cycle cost for LEO applications such as Space Station Freedom (30 year life). The primary drivers are transportation to orbit and battery cost.

IPV nickel/hydrogen technology was advanced at NASA Lewis and under Lewis contracts. Some of the advancements are as follows: (i) to use 26% potassium hydroxide electrolyte to improve cycle life and performance; (ii) to modify the state-of-the-art cell designs to eliminate identified failure modes and further improve cycle life, and (iii) to develop a lightweight nickel electrode to reduce battery mass, hence reduce launch cost and/or increase satellite payload.

The influence of KOH electrolyte concentration on cycle life was investigated at Hughes Aircraft Company under a NASA Lewis Contract. Hughes reported a breakthrough in LEO cycle life [2, 3]. Boiler plate cells containing 26% KOH were cycled for about 40 000 accelerated cycles at 80% DOD at 23 °C, compared with 3500 cycles for cells containing 31% KOH. These results are in the process of being validated using flight hardware and real time LEO test under a NASA Lewis Contract with the Naval Weapons Support Center (NWSC), Crane, IN.

The advanced design for an IPV nickel/hydrogen cell was conceived with the intention of improving cycle life at moderate-to-deep DOD (40 to 80%). The approach was to review IPV nickel/hydrogen cell designs and results of cycle life tests conducted in-house and by others to identify areas where improvements could result in a longer life [4–10]. The feasibility of the design was demonstrated using 6 Ah boiler plate cells [11]. The advanced design is in the process of being validated using 125 Ah flight cells and real time test under a NASA Lewis Contract with the NWSC, Crane, IN.

A lightweight nickel electrode using a thick, porous, fiber substrate has been evaluated in-house using boiler plate cells. The thickness was 80 mils (2 mm), porosity 90%, active material loading level 1.6 g/cm³ void volume.

In this report results of validation tests will be updated [12, 13].

Measurements and procedures

For both the 48 and 125 Ah cells, the quantities measured every 2.4 min for each cell during charge and discharge and their accuracies are: current ($\pm 2.0\%$), voltage ($\pm 0.001\%$), pressure ($\pm 1\%$), and temperature ($\pm 1\%$). Charge and discharge Ah capacities are calculated from current and time. Charge/discharge ratio (Ah into cell on charge to Ah out on discharge) is calculated from the capacities. Cell charge and discharge currents are calculated from the voltage measured across a shunt, using an integrated digital voltmeter. Cell pressure is measured with a strain gauge located on the cell dome. The temperature is measured using a thermistor located on the center of the pressure vessel dome. The thermistor is mounted by means of a heat sink compound to insure good thermal contact.

To verify the performance of lightweight nickel electrodes in boiler plate hardware, a nickel/hydrogen cell was assembled at NASA Lewis. The quantities measured during charge and discharge are: current ($\pm 2.0\%$), voltage ($\pm 0.001\%$), and time ($\pm 1\%$). The charge and discharge Ah and Wh are calculated from current and time on every scan. Every 18 s, the data are saved and stored to a data collector. The data can be retrieved for data and graphical output. The percent utilization is calculated by using the ratio of the measured discharge capacity to the theoretical calculated capacity based on the weight of the active material deposited. End-of-life failure is defined as the point where the discharge voltage degrades to 0.5 V.

For the 48 Ah cells, prior to cell final hydrogen gas adjustment, the nickel electrodes were positively charged, which results in a 0 atm hydrogen gas pressure. After completion

of acceptance testing the cells were discharged at the $C/10$ rate (4.8 A) to 0.1 V or less. The cells were shipped to NWSC, Crane, IN, where they were stored at 10 °C under trickle charge at $C/200$ for 31 days. After storage the discharge Ah capacity acceptance test was repeated. The capacity was measured after charging the cells at the $C/2$ rate (24 A) for 2.0 h, then $C/10$ for 6 h followed by a 0.5 h open-circuit stand. The discharge capacity was measured to 1.0 V at each of the following rates: $C/2$, C , $1.4C$, and $2C$.

Prior to undergoing cycle life testing, the capacity retention after a 72 h open-circuit stand (10 °C) was measured for each cell. For the cycle-life test the cells were connected electrically in series to form a six-cell pack. The cycle regime was a 90 min LEO orbit consisting of a 54 min charge at a constant $0.93C$ rate (44.7 A) followed by a 36 min discharge at a $1.33C$ rate (64 A). The charge/discharge ratio was 1.048. The DOD was 80% of name plate capacity (48 Ah). During the cycle-life test the cooling plate temperature was maintained at 10 ± 2 °C. Cell failure for this test was defined to occur when the discharge voltage degrades to 1.0 V during the course of the 36 min discharge.

For the 125 Ah cells, after completion of activation by the manufacturer, the precharge hydrogen pressure was set to 0 psig (14.5 psia) with the nickel electrodes in the fully discharged state. After completion of the acceptance testing the cells were discharged at the $C/10$ rate (12.5 A) to 0.1 V or less and the terminals were shorted. The cells were shipped to NWSC, Crane, IN, where they were stored at open circuit, and discharged at 0 °C for 52 days. After storage the discharge Ah capacity acceptance test was repeated. The capacity was measured after charging the cells at the $C/2$ rate (62.5 A) for 2 h, then $C/10$ for 6 h followed by a 0.5 h open-circuit stand. The discharged capacity was measured to 1.0 V for each of the following rates: $C/2$, C , $1.4C$, and $2C$.

Prior to undergoing cycle-life testing the capacity retention after a 72 h open-circuit stand (10 °C) was measured for each cell. For the cycle-life test the cells were connected electrically in series to form a six-cell pack. The cycle regime is a 90 min LEO orbit consisting of a 54 min charge at a constant $0.69C$ rate (87 A) followed by a 36 min discharge at a C rate (125 A). The charge/discharge ratio was 1.04. The DOD was 60% of name plate capacity (125 Ah). During the cycle-life test the cooling plate temperature was maintained at 10 ± 2 °C. Cell failure for this test was defined to occur when the discharge voltage degrades to 1.0 V during the course of the 36 min discharge.

The boiler plate cell was cycle-life tested using a 90 min cycle regime at 40% DOD. The continuous test regime consists of charging at a constant $0.48C$ rate for 55 min immediately followed by discharge at a constant $0.69C$ rate for 35 min. Cell capacities are measured every 1000 cycles, by charging at the C rate for 80 min followed by discharging at the $0.69C$ rate to 0.5 V. Failure of the cell occurs when the discharge voltage degrades to 0.5 V during the course of the constant current 35 min discharge at the $0.69C$ rate.

Experimental

Test facility

The facility is capable of testing 45 battery packs with maximum of 10 cells electrically connected in series per pack. Each pack has its own charge and discharge power supply controlled by a computer which is programmed to satisfy the particular

test requirements. During testing, each pack is scanned every 2.4 min to compare data such as voltage, temperature, and pressure with programmed limits. If a parameter is out of limit, an alarm will be initiated and a message will be typed out identifying the cell and parameter. The data are recorded on a 132 mB disc drive and if requested can be obtained in report form. The cell temperature during a test is controlled by a recirculating cooler that circulates a solution of water and ethylene glycol through a cooling plate.

Cell description

48 Ah flight cells

Six Air Force/Hughes recirculating design IPV nickel/hydrogen flight cells manufactured by Hughes are undergoing testing. Three of the cells contain 26% KOH electrolyte (test cells). The other three (control cells) are identical to the test cells but they contain 31% KOH. Both the test and control cells contain an equal number of components. The name plate capacity is 48 Ah. The cell is illustrated in Fig. 1. It consists of a stack of nickel electrodes, separators, hydrogen electrodes, and gas screen assembled in a non-back-to-back electrode configuration. In this configuration electrodes of different types directly face each other. The stack is packaged in a cylindrical pressure vessel, with hemispherical end caps. This is made of Inconel 718 and lined with zirconium oxide which serves as a wall wick. The components are shaped in a pineapple slice pattern. Like electrodes they are connected electrically in parallel. The separators consist of two layers of zircar, which extend beyond the electrodes to contact the wall wick. Hence, the electrolyte, which leaves the stack during cycling, will be wicked back. The gas screens are polypropylene. The nickel electrode consists of a dry sinter plaque containing a nickel screen substrate which was electrochemically impregnated by the alcoholic Pickett process [14].

125 Ah advanced flight cells

Six 125 Ah advanced design IPV nickel/hydrogen flight cells fabricated by Eagle-Picher, Joplin according to NASA Lewis specification are undergoing cycle-life testing. The nickel electrodes were fabricated at Eagle-Picher, Colorado Springs, and were impregnated with active material by the alcoholic Pickett process [14]. Three of the cells (test cells) contain all of the advanced design features as described in ref. 15. The other three cells (control cells) are the same as the test cells except they do not have catalyst on the wall wick. All six cells contain 26 rather than 31% KOH electrolyte.

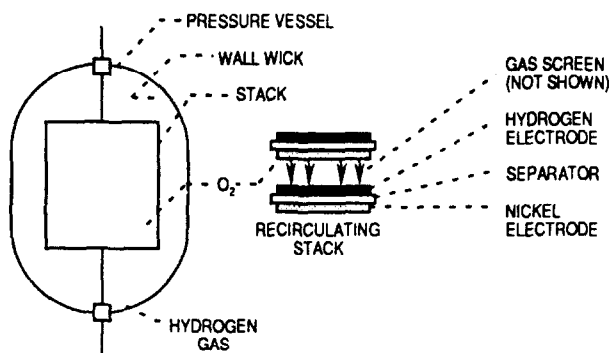


Fig. 1. Illustration of Hughes recirculation stack individual pressure vessel nickel/hydrogen cell.

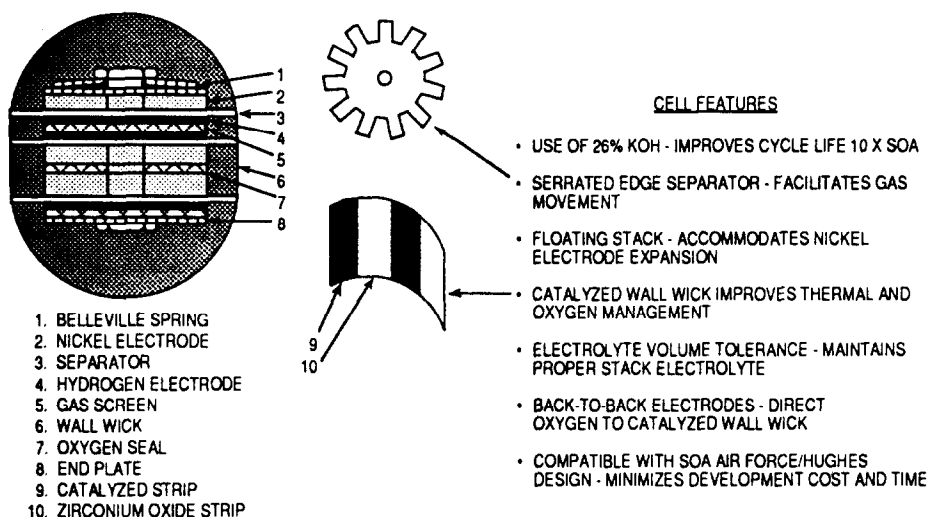


Fig. 2. NASA advanced design IPV nickel/hydrogen cell-catalyzed wall wick.

The test cell design is illustrated in Fig. 2. The new features of this design, which are not incorporated in the state-of-the-art Air Force/Hughes or COMSAT/Intelsat Cells, are: (i) use of 26 than 31% KOH electrolyte which improves cycle life [2, 3, 16]; (ii) use of a catalyzed wall wick located on the inside surface of the pressure vessel wall which chemically recombines oxygen generated at the end of charge and on overcharge with hydrogen to form water. State-of-the-art nickel/hydrogen cells recombine the oxygen on the catalyzed hydrogen electrode surface in the stack. The catalyzed wall wick should improve oxygen and thermal management [17]; (iii) use of serrated edge separators to facilitate gaseous oxygen and hydrogen flow within the cell, while still maintaining physical contact with the wall wick for electrolyte management, and (iv) use of a floating rather than fixed stack (SOA) to accommodate nickel electrode expansion due to charge/discharge cycling. This is accomplished by use of Belleville disc springs located at each end of the stack. The significant improvements resulting from these innovations are extended cycle life, enhanced oxygen, thermal and electrolyte management, and accommodation of some of the nickel electrode expansion.

Lightweight nickel electrode

The lightweight nickel electrodes evaluated were fabricated from Fibrex nickel fiber substrates. The substrates contain 50% nickel fibers, 35% nickel powder and 15% cobalt powder. The porosity was 90% and the thickness was 80 mils (2 mm). They were electrochemically impregnated by Eagle-Picher using the aqueous process to a loading level of 1.6 g/cm³.

Cell description

For testing lightweight nickel electrodes

The cycle test was conducted using a boiler plate cell with a 5 cm×5 cm active area. The components of the cell consist of a stack of nickel electrode, separator, hydrogen electrode, and gas screen. The nickel electrode is made from an 80 mil (2 mm) thick, 90% porous Fibrex nickel electrode loaded to 1.6 g/cm³ void volume.

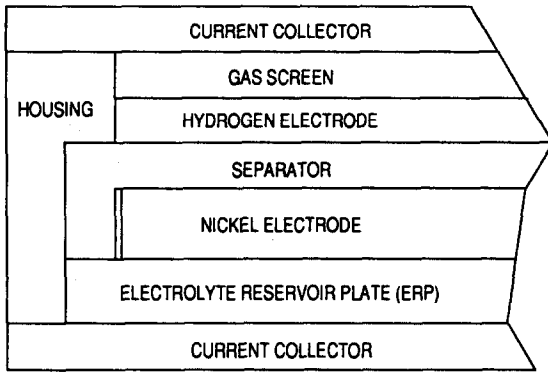


Fig. 3. Cross-sectional unit of the nickel/hydrogen cell.

The separator consists of three layers of 6 mil (0.13 mm) thick beater treated asbestos separator. The hydrogen electrode was made by Life Systems, Inc., and consists of a mixture of platinum and Teflon applied to a gold-plated nickel screen. The gas screen, located behind the hydrogen electrode, is 60 mil (1.3 mm) thick nickel Exmet which was compressed to 40 mil (1 mm) to fit into the cavity designed for the hydrogen electrode and gas screen. An electrolyte reservoir plate (ERP), which is incorporated into the cell, is made of 125 mil (3.2 mm) thick foam metal. The current collectors are gold-plated nickel. A graphic representation of the unit cell cross section is shown in Fig. 3. After assembly, the entire stack is vacuum-filled with 26% KOH electrolyte. The electrolyte is allowed to stand in the stack overnight, then the excess electrolyte is drained. The stack is placed in a pressure vessel which is evacuated and filled with hydrogen to 3.4 atm (50 psi).

Results and discussion

48 Ah flight cells

Storage test

The nickel/hydrogen battery could undergo a planned or unplanned storage due to delays prior to launch. This may have an effect on performance. The influence of storage (31 days, trickle charged at $C/200$, 10 °C) on the capacity of the 48 Ah IPV nickel/hydrogen flight cells containing 26 and 31% KOH electrolyte is shown in Fig. 4. The spread in the data indicates there is no significant capacity loss after 31 days for either the 26 or 31% KOH cells.

Performance test

A comparison of the average discharge voltage (three cells) as a function of time for the cells containing 26 and 31% KOH was made and is shown in Fig. 5. The voltage for the 26% KOH cells is higher than for the 31% KOH cells up to about an 82% DOD. The discharge rate was 1.4C (67.2 A) and the cell temperature was maintained at 10 °C. The Ah capacity for these cells is shown in Table 1 (1.4C, 10 °C). The capacity on the average for the 26% KOH cells was about 10% lower than the 31% KOH cells. The trade-off for this relatively small decrease in initial capacity is a significant increase in cycle life. It should be noted that the data in Table 1 are for a 100% DOD. In an actual application the DOD will be much less.

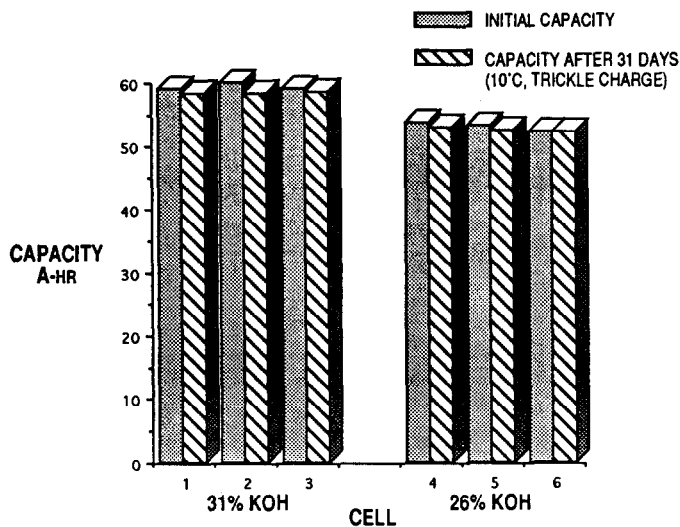


Fig. 4. Effect of storage on capacity of 48 Ah Hughes IPV nickel/hydrogen flight cells.

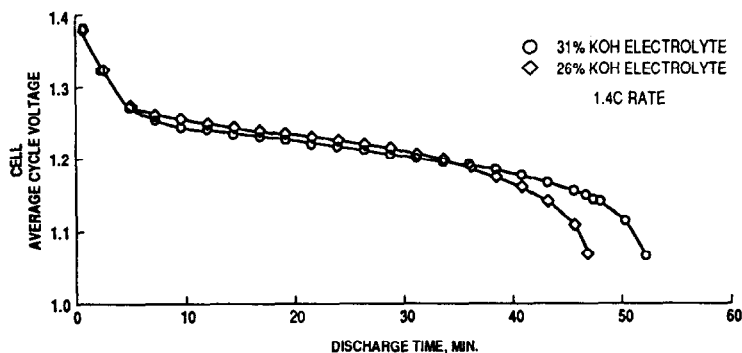


Fig. 5. Comparison of Hughes 49 Ah IPV nickel/hydrogen flight cells containing 26 and 31% KOH electrolyte.

TABLE 1

Capacity of Hughes flight cells containing 26 and 31% KOH electrolyte

Cell no.	Capacity ^a (Ah)	Concentration KOH (%)
1	59.0	31
2	59.9	31
3	59.0	31
4	53.8	26
5	53.2	26
6	52.3	26

^aDischarge at 1.4C rate, 10 °C.

For instance the DOD for Space Station Freedom will be about 35%. In this operating region the cells containing 26% KOH have a higher discharge voltage, and still have adequate capacity reserve.

Cycle test

The influence of LEO cycling at 80% DOD on the end-of-discharge voltage for the 48 Ah IPV nickel/hydrogen flight cells containing 26% KOH is summarized in Fig. 6. The three cells containing 26% KOH failed on the average at cycle 19 500 (cycle 15 314, 19 518, and 23 659). The influence of cycling on the end-of-charge pressure for the 26% KOH cells is shown in Fig. 7. The pressure increase per 1000 cycles is 23.3 psi. The pressure increase could be indicative of nickel plaque corrosion which converts nickel to active material. The increase in pressure will result in a shift in the beginning of life state-of-charge versus pressure curve.

The influence of LEO cycling at 80% DOD on the end-of-discharge voltage for the cells containing 31% KOH is shown in Fig. 8. The three cells containing 31% KOH failed on the average at cycle 6400 (cycles 3729, 4165 and 11 355). The failure mode for each cell was characterized by degradation of discharge voltage to 1.0 V. No cell failed due to an electrical short. A comparison of the discharge curve at the beginning and end of life for cell 1, which failed at cycle 3729, is shown in Fig. 9. This information also shows a voltage degradation. The Ah capacity decrease for cell 1 was about 33% (1.4C rate, 10 °C), for cell 2 33%, and for cell 3 36%. The influence of cycling on the end-of-charge pressure for the 31% KOH cells is shown in Fig. 10. The pressure change can be correlated with the discharge voltage change due to cycling. The pressure increase per 1000 cycles is 23.3 psi. The pressure increase is the same as for the 26% KOH.

The cycle life of the cells containing 26% KOH was a factor of 3 to 4 better than those with 31% KOH. The superior performance of the 26% KOH cells compared with the 31% cells is in agreement with boiler plate cell results reported previously

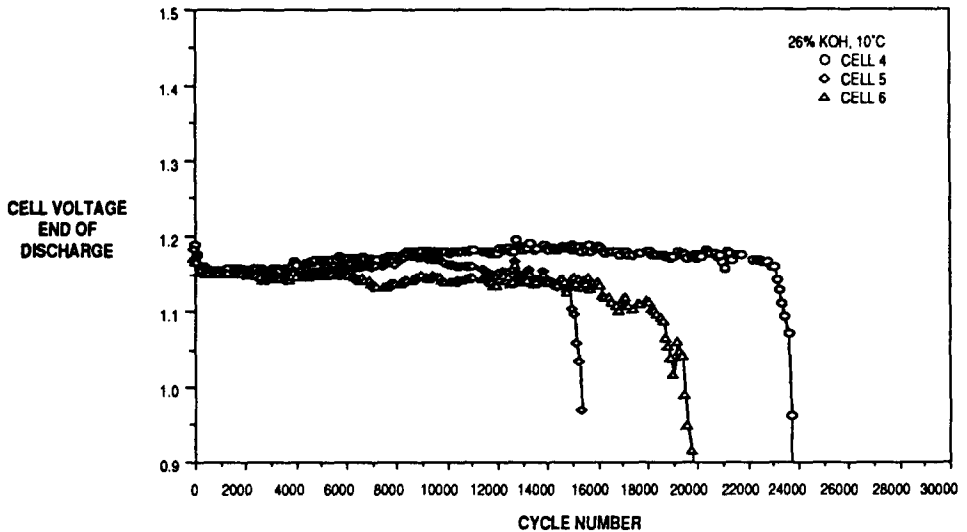


Fig. 6. Effect of LEO cycling at 80% DOD on 48 Ah IPV Hughes flight cells containing 26% KOH electrolyte, 10 °C.

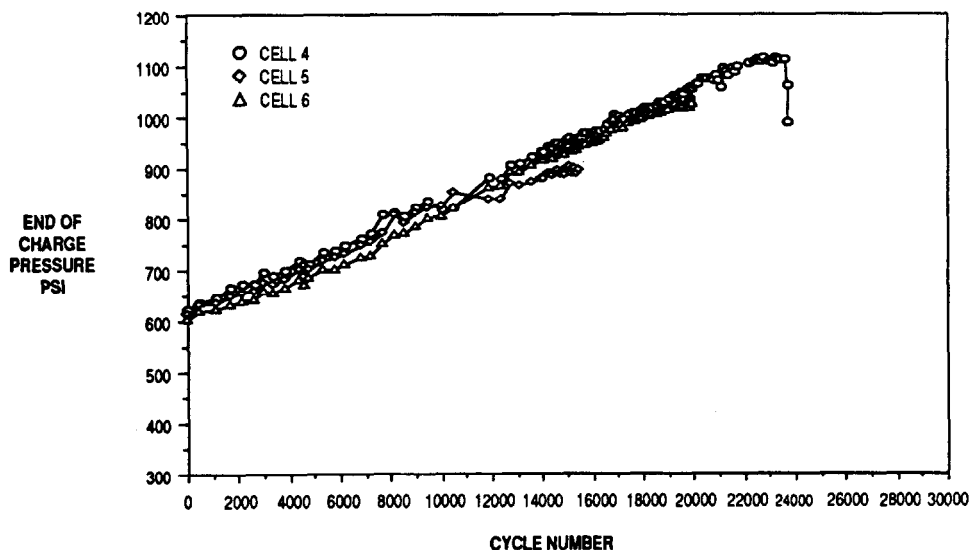


Fig. 7. Effect of LEO cycling at 80% DOD on 48 Ah IPV Hughes flight cells containing 26% KOH.

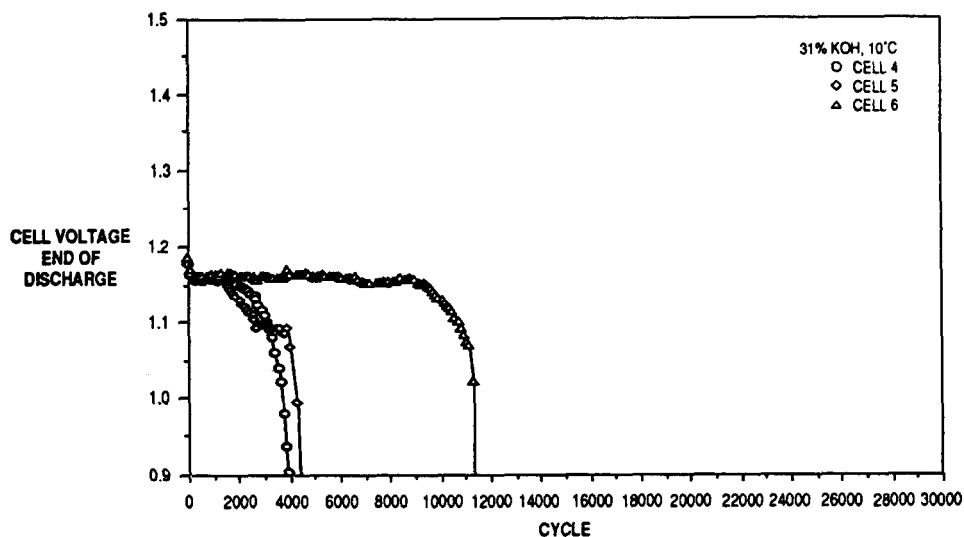


Fig. 8. Effect of LEO cycling at 80% DOD on Hughes flight cells containing 31% KOH electrolyte, 10 °C.

cells (2 and 3). It is attributed to crystallographic change of active material [16]. γ -NiOOH is converted to β -NiOOH in 26% KOH. β -NiOOH has a lower capacity, but longer life.

Destructive physical analysis

Destructive physical analysis (DPA) of all three of the 31% KOH cells was completed and documented at Hughes under a NASA Lewis contract [18]. DPA of

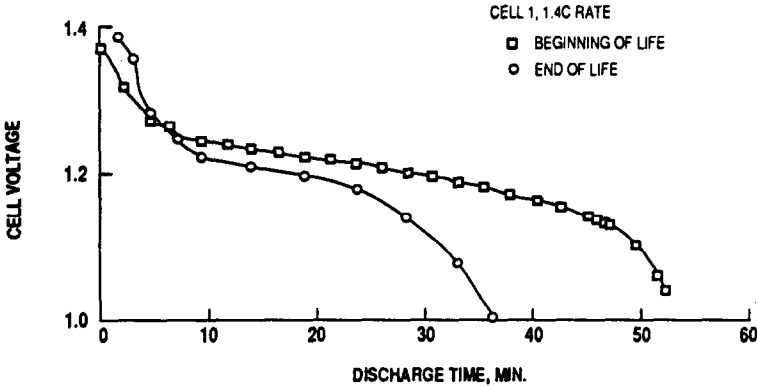


Fig. 9. Comparison of Hughes 48 Ah IPV nickel/hydrogen flight cells containing 31% KOH electrolyte.

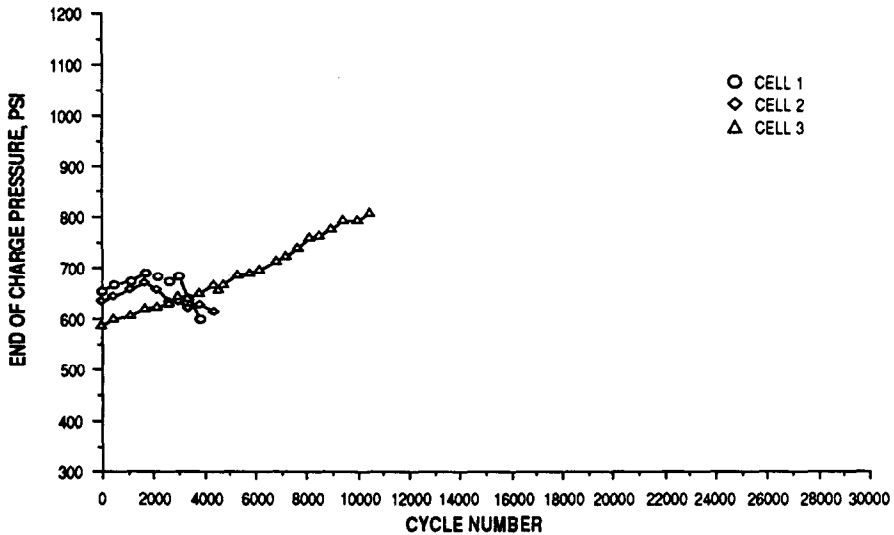


Fig. 10. Effect of LEO cycling at 80% DOD on Hughes flight cells containing 31% KOH.

the 26% cells is in process. A summary of the DPA results of the 31% KOH cells is as follows: all three cells failed during cycling due to a decrease in voltage and nickel electrode capacity. The capacity decrease was confirmed by measuring nickel electrode capacity in flooded electrolyte cells. Some observations which could cause the capacity decrease are nickel electrode expansion, rupture and corrosion of the nickel electrode substrate, active material redistribution, and accumulation of electrochemically undischarged active material with cycling. Cell 3 appears to have failed by gradual wear-out due to these changes. Some of the electrodes from cells 1 and 2 showed a premature capacity fading which was responsible for early failure. However, chemical analysis of these electrodes did not show anomalous results. The mechanism of the premature capacity fading is not fully understood by the present DPA. No cells failed due to an electrical short. All cells showed some increase in internal resistance

after the cycle test; however, this increase itself does not appear to be the direct cause of failure. All cells showed a decrease in discharge voltage and an increase in charge voltage after the cycle test.

125 Ah advanced flight cells

Cell performance

For a representative 125 Ah advanced catalyzed wall wick nickel/hydrogen flight battery cell the voltage and pressure during charge and discharge are shown in Fig. 11 (beginning of life). The discharge rate was $0.69C$ (87 A) and the temperature was a nominal 10°C . The mid-discharge voltage was 1.248 V. The pressure, as expected, varies linearly with the state-of-charge. It should be noted, however, that the pressure could increase with charge/discharge cycling causing a shift in the state-of-discharge curve.

The effect of discharge rate on Ah capacity for a representative cell of each type is shown in Fig. 12. The capacity decreased slightly (1%) over the range of $C/2$ to $1.4C$, after which point it decreased rapidly. In a nickel/hydrogen cell the gaseous hydrogen comes into contact with the nickel electrodes resulting in a capacity loss due to self-discharge. The capacity retention of the cells after a 72 h open-circuit stand at 10°C is shown in Fig. 13. The data show no significant difference in capacity retention between the catalyzed and noncatalyzed wall wick cells. The capacity retention for the catalyzed wall wick cells on the average is 84% and for the noncatalyzed wall wick cells is 85%.

Storage test

The effect of storage (52 days, discharged, open circuit, 0°C) on the capacity of the six 125 Ah flight IPV nickel/hydrogen cells is summarized in Fig. 14. The spread in the data shows no significant capacity loss for either the catalyzed or noncatalyzed wall wick cells due to the 52 day storage. Actually, there was a slight average increase in capacity for both the catalyzed and noncatalyzed wall wick cells.

Cycle test

The influence of LEO cycling at 60% DOD on the end-of-discharge voltage for the 125 Ah catalyzed wall wick IPV nickel/hydrogen flight cells is summarized in

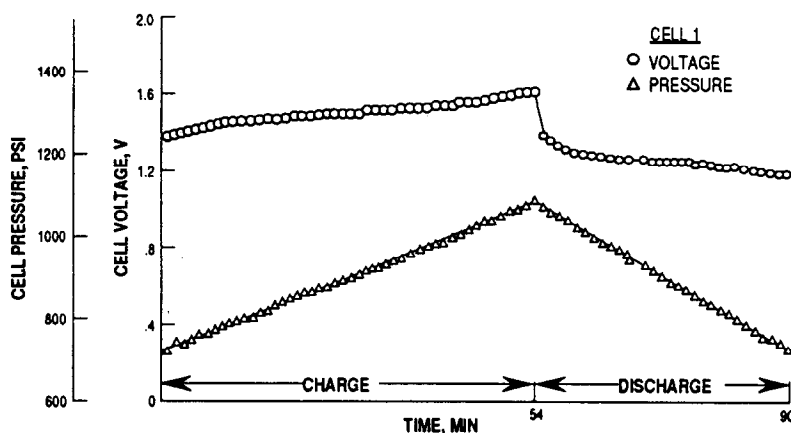


Fig. 11. Cell voltage and pressure during charge and discharge for a representative 125 Ah advanced catalyzed wall wick IPV nickel/hydrogen flight battery cell.

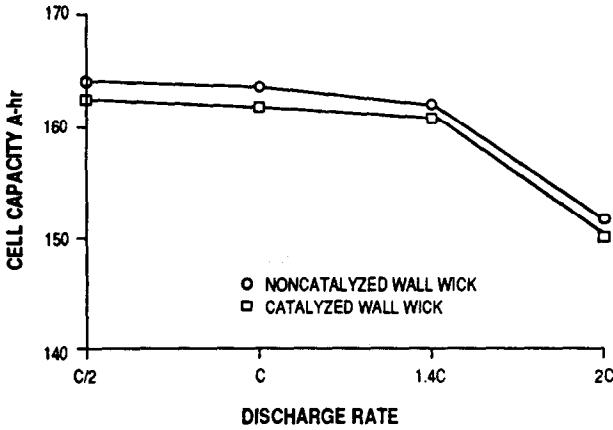


Fig. 12. Comparison of Eagle-Picher 125 Ah nickel/hydrogen cells catalyzed and noncatalyzed wall wick.

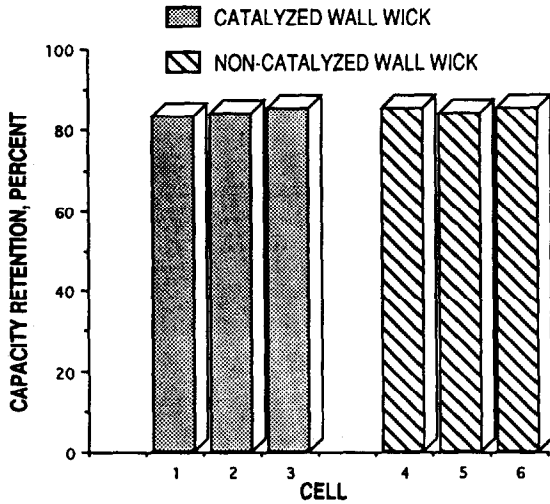


Fig. 13. Capacity retention of 125 Ah Eagle-Picher advanced IPV nickel/hydrogen flight cells after 72 h open-circuit stand.

Fig. 15. After 22 694 cycles there has been no cell failure in the continuing test. The influence of cycling on the end-of-charge pressure for the catalyzed wall wick cells is shown in Fig. 16. No pressure for cell 2 is available because the cell had a bad strain gauge. For cells 1 and 3 the pressure increased relatively rapidly up to about cycle 1400, then decreased. The average pressure increase at cycle 1400 is about 11% higher than at the beginning of life.

The influence of LEO cycling at 60% DOD on the end-of-discharge voltage for the 125 Ah noncatalyzed wall wick IPV nickel/hydrogen flight cells is shown in Fig. 17. All three of the noncatalyzed wall wick cells failed (cycles 9588, 13 900, and

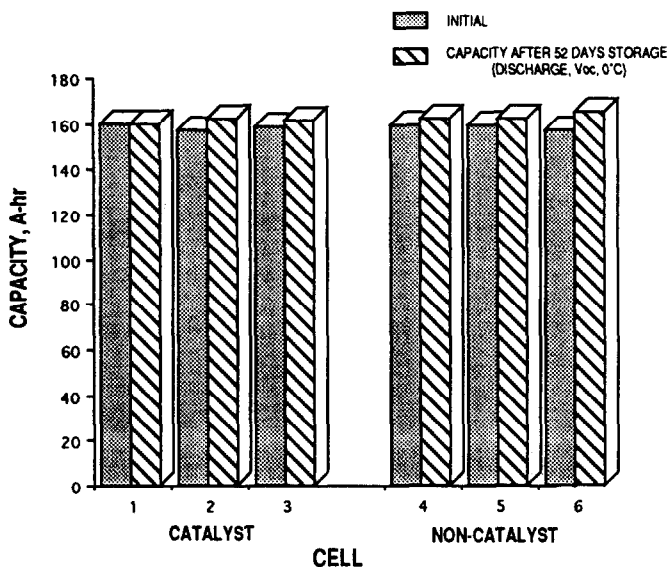


Fig. 14. Effect of storage on capacity of 125 Ah Eagle-Picher advanced IPV nickel/hydrogen flight cells, catalyzed and noncatalyzed wall wick, 26% KOH.

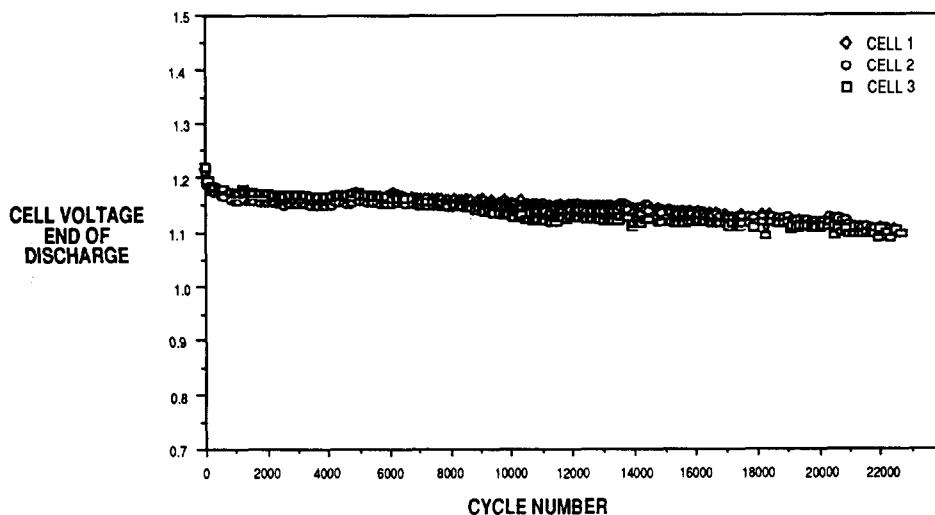


Fig. 15. Effect of LEO cycling on 125 Ah NASA Lewis advanced catalyzed wall wick IPV nickel/hydrogen cells manufactured by Eagle-Picher, 26% KOH, 60% DOD, 10 °C.

20 575). The failure was characterized by degradation of end-of-discharge voltage to 1.0 V. The cells did not fail due to an electrical short. The influence of cycling on the end-of-charge pressure for the noncatalyzed wall wick cells is shown in Fig. 18. The pressure for the three cells increased up to about cycle 2000 then decreased.

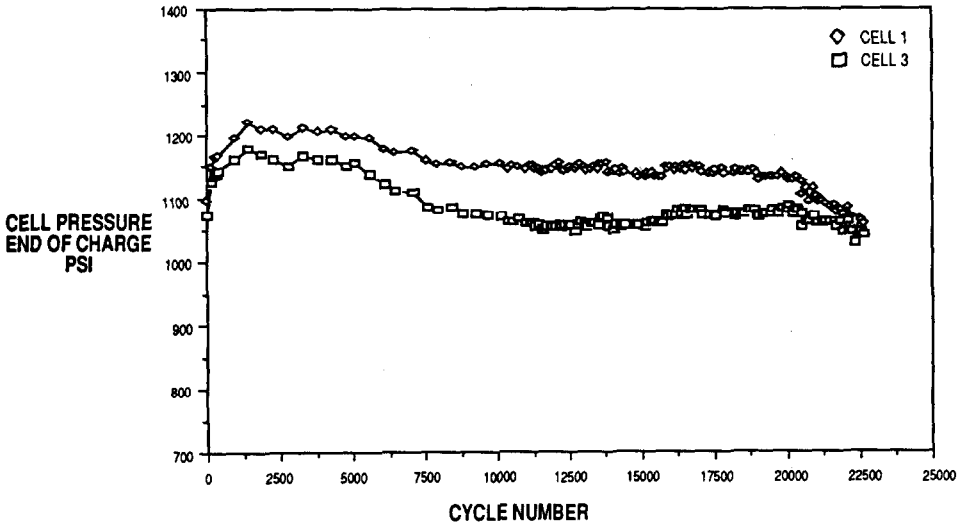


Fig. 16. Effect of LEO cycling on 125 Ah NASA Lewis advanced catalyzed wall wick IPV nickel/hydrogen cells manufactured by Eagle-Picher, 26% KOH, 60% DOD, 10 °C.

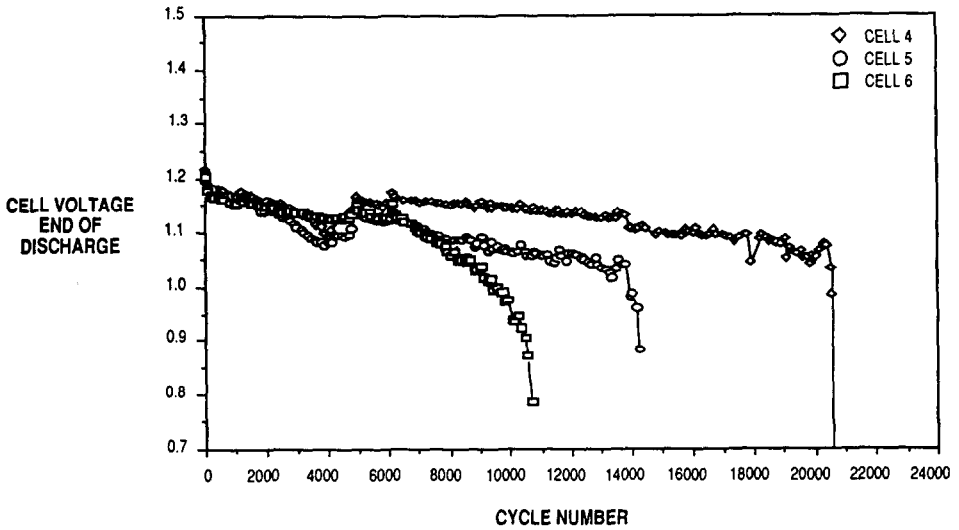


Fig. 17. Effect of LEO cycling on 125 Ah NASA Lewis advanced noncatalyzed wall wick IPV nickel/hydrogen cells manufactured by Eagle-Picher, 26% KOH, 60% DOD, 10 °C.

The average pressure increase at cycle 2000 is about 9% higher than at the beginning of life.

The cycle-life testing will continue until cell failure. A post-cycle teardown and failure analysis will be conducted to evaluate the cause of failure. This information will be used to affect further improvements.

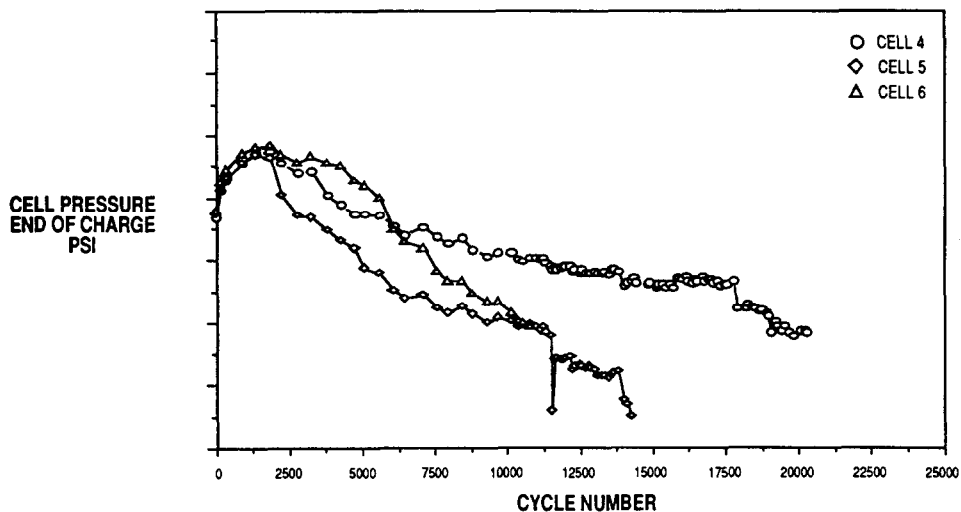


Fig. 18. Effect of LEO cycling on 125 Ah NASA Lewis advanced noncatalyzed wall wick IPV nickel/hydrogen cells manufactured by Eagle-Picher, 26% KOH, 60% DOD, 10 °C.

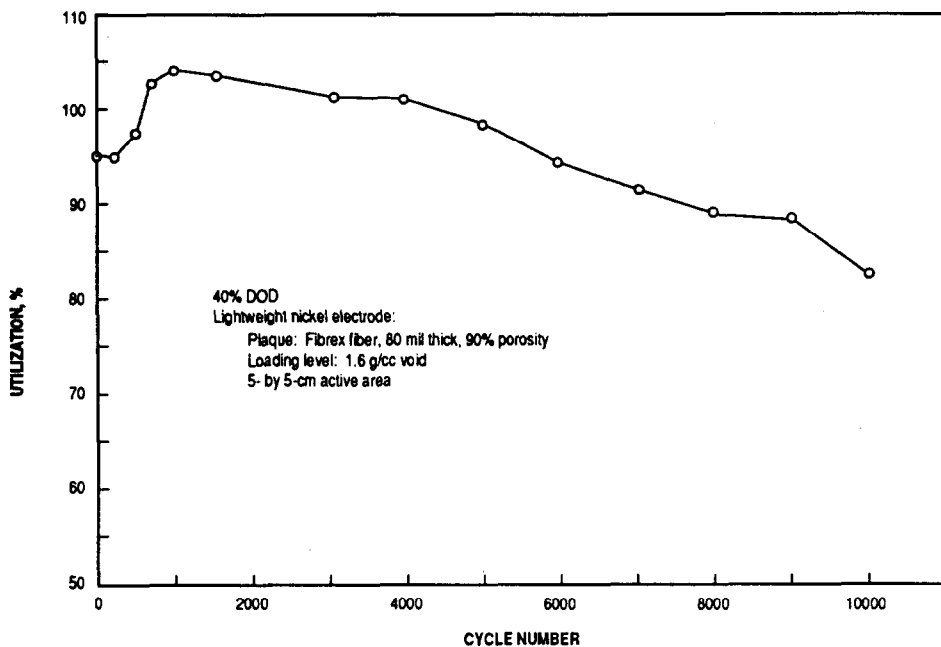


Fig. 19. Utilization vs. cycle number of a nickel/hydrogen cell using a Fibrex nickel electrode.

Boiler plate cell

For testing lightweight nickel electrodes

The cell cycled for 10 000 cycles, as shown in Fig. 19, before the test was terminated. The effect of cycling on the end-of-discharge voltage is shown in Fig. 20. An end-of-

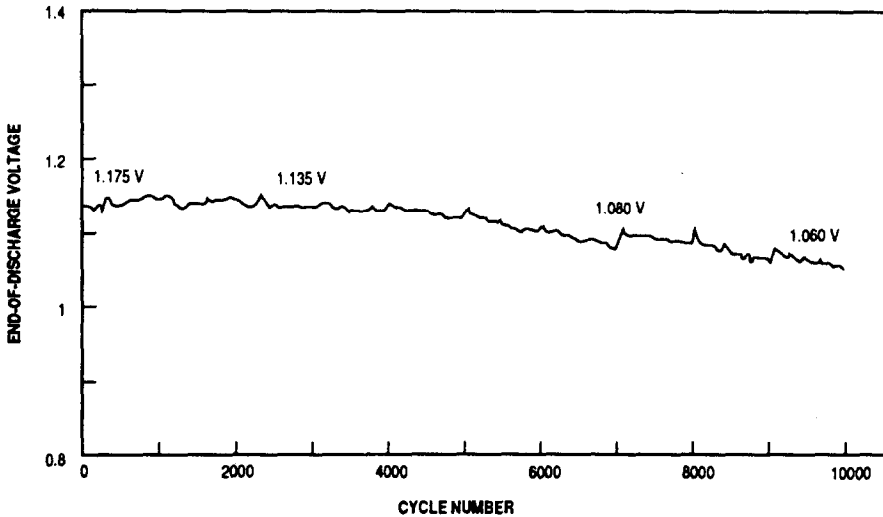


Fig. 20. End-of-discharge voltage vs. number of cycles for a nickel/hydrogen cell using a Fibrex nickel electrode.

discharge voltage of about 1.175 V is observed for the first 1000 cycles. The average end-of-discharge voltage gradually dropped to about 1.060 V at 9000 cycles and remained constant until the end of the cycle test.

Final characterization testing will be conducted and will be reported later. Failure analysis will also be conducted to evaluate the cause for failures.

Conclusions

A breakthrough in the LEO cycle life of individual pressure vessel nickel/hydrogen battery cells was reported. The cycle life of boiler plate cells containing 26% KOH electrolyte was about 40 000 accelerated LEO cycles at 80% DOD compared with 3500 cycles for cells containing 31% KOH. Results of the boiler plate cell tests have been validated at NWSC, Crane, IN. Forty-eight Ah flight cells containing 26 and 31% KOH have undergone real time LEO cycle-life testing at an 80% DOD, 10 °C. The three cells containing 26% KOH failed on the average at cycle 19 500. The three cells containing 31% KOH failed on the average at cycle 6400.

Validation testing of NASA Lewis 125 Ah advanced design IPV nickel/hydrogen flight cells is also being conducted at NWSC, Crane, IN under a NASA Lewis contract. This consists of characterization, storage, and cycle-life testing. There was no capacity degradation after 52 days of storage with the cells in the discharged state, on open circuit, 0 °C, and a hydrogen pressure of 14.5 psia. The catalyzed wall wick cells have been cycled for over 22 694 cycles with no cell failures in the continuing test. All three of the noncatalyzed wall wick cells failed (cycles 9588, 13 900 and 20 575).

Cycle-life test results of the Fibrex nickel electrode have demonstrated the feasibility of an improved nickel electrode giving a higher specific energy nickel/hydrogen cell. A nickel/hydrogen boiler plate cell using an 80 mil (2 mm) thick, 90% porous Fibrex nickel electrode has been cycled for 10 000 cycles at 40% DOD.

References

- 1 L. Miller, *Proc. 23rd Intersociety Energy Conversion Engineering Conf., Denver, CO, USA, July 31–Aug. 5, 1988*, Vol. 2, American Society of Mechanical Engineers, New York, pp. 489–492.
- 2 H.S. Lim and S.A. Verzwylt, *J. Power Sources*, 22 (1988) 213–220.
- 3 H.S. Lim and S.A. Verzwylt, *J. Power Sources*, 29 (1990) 503–519.
- 4 E. Adler, T. Duranti, P. Frisch, T. Jacwicz, H. Rogers, L. Samoss, S. Stadnick and L. Tinker, Nickel–hydrogen battery advanced development program, *AFWAL-TR-80-2044*, Hughes Aircraft Company, 1980.
- 5 D. Warnock, Life test of 50 Ah NiH₂ battery, in G. Halpert (ed.), *The 1981 Goddard Space Flight Center Workshop, Greenbelt, MA, USA, Nov. 17–19, 1981*, NASA CP-2217, 1982, pp. 487–500.
- 6 J. J. Smithrick, *Proc. 18th Intersociety Energy Conversion Engineering Conf., Orlando, FL, USA, Aug. 21–26, 1983*, Vol. 4, American Institute of Chemical Engineers, New York, pp. 1535–1542.
- 7 D.H. Fritts, *J. Power Sources*, 6 (1981) 171–184.
- 8 D.F. Pickett, H.H. Rogers, L.A. Tinker, C.A. Bleser, J.M. Hill and J.S. Meador, *Proc. 15th Intersociety Energy Conversion Engineering Conf., Miami, FL, USA, Aug. 18–23, 1985*, Vol. 3, American Institute of Aeronautics and Astronautics, New York, pp. 1918–1924.
- 9 V.C. Mueller, in D. Baer and G.W. Morrow (eds.), *The 1983 Goddard Space Flight Center Battery Workshop, NASA CP-2331, Greenbelt, MA, USA, Nov. 15–17, 1983*, pp. 523–538.
- 10 K.M. Abbey and D.L. Britton, Electrolyte management in porous battery components – Static measurements, *NASA TM-83073*, 1982.
- 11 J.J. Smithrick, in L. J. Pearce (ed.), *Power Sources 11: Research and Development in Non-Mechanical Electrical Power Sources*, International Power Sources Symposium Committee, Leatherhead, UK, 1986, pp. 215–226; *NASA TM-87282*.
- 12 J.J. Smithrick and S.W. Hall, in D.C. Black (ed.), *Proc. 26th Intersociety Energy Conversion Engineering Conf., 1991*, Vol. 3, American Nuclear Society, 1991, pp. 276–281.
- 13 J.J. Smithrick and S.W. Hall, in D.L. Black (ed.), *Proc. 25th Intersociety Energy Conversion Engineering Conf., Boston, MA, USA, Aug. 4–9, 1991*, Vol. 3, American Nuclear Society, 1991, pp. 311–317.
- 14 D.F. Pickett, *US Patent No. 3 827 911* (Aug. 1974).
- 15 J.J. Smithrick, M.A. Manzo and O. Gonzalez-Sanabria, *Proc. 19th Intersociety Energy Conversion Engineering Conf., San Francisco, CA, USA, Aug. 19–24, 1984*, Vol. 1, American Nuclear Society, New York, 1984, pp. 631–635; *NASA TM-83643*.
- 16 H.S. Lim and S.A. Verzwylt, in D.A. Corrigan and A.A. Zimmerman (eds.), *Proc. Symp. Nickel–Hydroxide Electrodes, Hollywood, FL, USA, Dec. 16–18, 1989*, Vol. 90-4, The Electrochemical Society, Pennington, NJ, USA, 1990, pp. 341–355.
- 17 O.D. Gonzalez-Sanabria, in D.Y. Goswami (ed.), *Proc. 23rd Intersociety Energy Conversion Engineering Conf., Denver, CO, USA, July 31–Aug. 5, 1989*, Vol. 2, American Society Mechanical Engineers, New York, 1988, pp. 453–456.
- 18 H.S. Lim, G.R. Zelter, T.T. Smithrick and S.W. Hall, in D.L. Black (ed.), *Proc. 26th Intersociety Energy Conversion Engineering Conf., Boston, MA, USA, Aug. 4–9, 1991*, Vol. 3, American Nuclear Society, 1991, pp. 304–310.